Molecular Crystals and Liquid Crystals Science and Technology. Section A. Molecular Crystals and Liquid Crystals

Publication details, including instructions for authors and subscription information:
http://www.tandfonline.com/loi/gmcl19

Dynamics of the Reorientation of a Ferroelectric Liquid Crystal Under an Electric Field Studied by Time-Resolved Optical Waveguide Spectroscopy

M. Mitsuishi [a] , S. Ito [a] , M. Yamamoto [a] , T. Fischer [b] & W. Knoll [c d]

[a] Department of Polymer Chemistry, Graduate School of Engineering, Kyoto University, Sakyo, Kyoto, 606-01, Japan

[b] Fakultät für Physik, Universität Leipzig, Linnéstraβe 5, D-04103, Leipzig, Germany

[c] Max-Planck-Institut für Polymerforschung, Ackermannweg 10, D-55128, Mainz, Germany

[d] The Institute of Physical and Chemical Research (RIKEN), Frontier Research Program, 2-1 Hirosawa, Wako, Saitama, 351-01, Japan

Version of record first published: 04 Oct 2006

To cite this article: M. Mitsuishi, S. Ito, M. Yamamoto, T. Fischer & W. Knoll (1997): Dynamics of the Reorientation of a Ferroelectric Liquid Crystal Under an Electric Field Studied by Time-Resolved Optical Waveguide Spectroscopy, Molecular Crystals and Liquid Crystals Science and Technology. Section A. Molecular Crystals and Liquid Crystals, 308:1, 001-026

To link to this article: http://dx.doi.org/10.1080/10587259708045092

Mol. Cryst. Liq. Cryst., 1997, Vol. 308, pp. 1–26
Reprints available directly from the publisher
Photocopying permitted by license only

Dynamics of the Reorientation of a Ferroelectric Liquid Crystal Under an Electric Field Studied by Time-Resolved Optical Waveguide Spectroscopy

M. MITSUISHI[a], S. ITO[a], M. YAMAMOTO[a,*],
T. FISCHER[b] and W. KNOLL[c]

[a]*Department of Polymer Chemistry, Graduate School of Engineering, Kyoto University, Sakyo, Kyoto 606-01, Japan;* [b]*Fakultät für Physik, Universität Leipzig, Linnéstraße 5, D-04103 Leipzig, Germany;* [c]*Max-Planck-Institut für Polymerforschung, Ackermannweg 10, D-55128 Mainz, Germany, and The Institute of Physical and Chemical Research (RIKEN), Frontier Research Program, 2-1 Hirosawa, Wako, Saitama 351-01, Japan*

(Received 28 February 1997; In final form 22 April 1997)

The dynamic structure and molecular reorientation of a ferroelectric liquid crystal induced by an alternating electric field have been investigated by time-resolved optical waveguide spectroscopy (TROWS) in which the transient waveguide mode patterns were recorded as a function of both time and angle of incidence of a probe beam. A ferroelectric liquid crystal, 4-(2S, 3S)-[2-chloro-3-methylpentanoyloxy]-4′-octyloxybiphenyl (3M2CPOOB) was utilized, which showed a fast response to an external electric field in the order of a microsecond. Under a high electric field, it forms the so-called bookshelf structure in which the director of 3M2CPOOB is tilted by 22.5° away from the smectic layer normal in the SmC* phase. Time-resolved waveguide mode patterns were successfully obtained with a time-resolution of 1.0 μs which enabled us to determine the transient features of dielectric tensor of 3M2CPOOB molecules in three dimensional coordinate system. A model that the molecular reorientation coupled with the layer buckling and the rotation around the cone was proposed from the quantitative analysis of the TROWS data.

Keywords: Ferroelectric liquid crystal; guided optical wave; TROWS

*Author to whom correspondence should be addressed.

1. INTRODUCTION

The electro-optic effect in ferroelectric liquid crystals (FLCs) has received significant attention because of its potential for fast switching and bistability as first reported by Clark and Lagerwall [1]. Various kinds of techniques, *e.g.*, the polarised optical transmission technique [2–4], X-ray diffraction analysis [5, 6], *etc.*, have been used in order to investigate these unique properties of FLC. The specific layer structure has been revealed by complementary works based on these experimental data and theoretical models [6]. These findings have been reviewed in some textbooks [7].

As a probe for the layer structure in more detail, guided optical waves have proved to be a powerful tool for detecting the optical properties in the dielectric medium [8–10]. The guided optical modes [11] in which the light propagates through the dielectric medium are very sensitive to tiny changes in the dielectric tensor and the thickness of the whole layer. They can be excited both with TE and TM light, *i.e.*, *s*- and *p*-polarized light, respectively. Elston and Sambles *et al.* [12–16] have extensively investigated the molecular orientation in the liquid crystal (LC) layer using the technique based on guided optical waves. Comparing the angle-dependent experimental reflectivity and a theoretical curve calculated for the model as stacked layers by the scattering matrix method [17], they found some characteristic layer structures of the FLC in the SmC* phase, *e.g.*, a half-splayed structure [12] and a chevron structure [13]. Ito *et al.* [18] showed another advantage of guided optical waves as a probing technique for the switching process of the FLC layer using modulated reflectivities with single and double frequencies with respect to the applied electric field frequency. It is difficult for the transmission technique to characterize the dielectric tensor profile as fully as the guided optical wave technique [13].

For the last decade, the real-time observation of the switching process of the FLC molecules has been reported using not only time-resolved transmission measurements [19–22], but also time-resolved FT-IR spectroscopy [23, 24]. The former technique gives us information about the kinetics of the FLC as a director rotation around the cone. For example, Fukuda *et al.*, elucidated the reorientation mechanism of the FLC from the stroboscopic observation [20, 25]. There are two kinds of mechanism; one is a fast response, with a simultaneous uniform reorientation throughout the whole FLC layer, while the other is a slow response that includes the nucleation of domains caused by the discontinuity of the director, *i.e.*, two surface and one internal disclination. On the other hand, the latter technique is able to provide information about the transient orientation of the IR active units in the FLC molecules at the sub-molecular level. To our knowledge, the im-

portant aspect of the reorientation in the SmC* phase obtained from time-resolved FT-TR spectroscopy is that the FLC molecules reorient "as a rigid core" during the reorientation, *i.e.*, both the rigid and flexible groups reorient simultaneously. Besides, the hindered rotation of the carbonyl group, which is responsible for the ferroelectricity, was observed under an electric field using infrared dichroism (not time-resolving) [26,27]. As another method, time-resolved Raman spectroscopy [28] has been used to study the response of nematic liquid crystals, but not the one of FLC.

Time-resolving is also one of the fascinating possibilities of guided optical waves; high time-resolution in the order of a nanosecond can be expected involving high accuracy for the determination of the optical thickness and dielectric constants of the LC layer. From this point of view, we developed a novel technique, time-resolved optical waveguide spectroscopy (TROWS), which provides reflectivities as a function of both the angle of the incidence and the time after applying an electric field [29]. We have demonstrated the usefulness of TROWS in a previous investigation on the dynamics of a nematic liquid crystal [30].

In this article, we report the dynamics of FLC molecules in the course of switching between the bistable states under an alternating external electric field. Using TROWS, one is able to observe the real-time switching process of the FLC molecules with a 1.0 μs time-resolution through the recording of the transient waveguide mode patterns. The quantitative analysis of the experimental data was performed using some simplifying approximations, whereby the dynamic structures and reorientation kinetics of the FLC molecules under the alternating electric fields have been discussed in detail.

2. EXPERIMENTAL

A ferroelectric liquid crystal 4-(2S, 3S)-[2-chloro-3-methylpentanoyloxy]-4′-octyloxybiphenyl (3M2CPOOB) was used in the current study, the molecular structure of which is as follows:

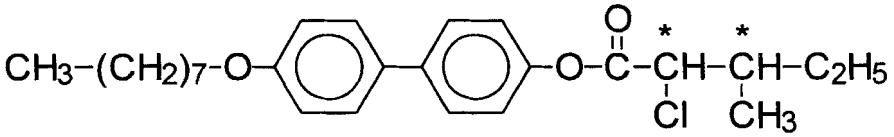

STRUCTURE 1

The synthesis of this material has been reported elsewhere [31,32].

The 3M2CPOOB molecule has two chiral groups which may be responsible for its large spontaneous polarization [31] and its fast response to an external electric perturbation [33]. On cooling the temperature from the isotropic phase, the simple sequence of phase transition temperatures was observed using a polarized microscope:

$$\text{Iso}—65^{\circ}\text{C}—\text{SmA}—55^{\circ}\text{C}—\text{SmC}^{*}—49^{\circ}\text{C}—\text{Cryst.}$$

Figure 1 illustrates the optical cell for the measurement of waveguide mode patterns. The details of the optical cell fabrication and the measurement procedure have been published elsewhere [31]. Two glass substrates (BK-7) were coated with a thin layer of gold (~ 40 nm) in a vacuum chamber ($\sim 2.0 \times 10^{-6}$ torr). On the gold layers were coated the layers of polyimide (PI, AL1524H, Japan Synthetic Rubber Co.) with a spinner, which

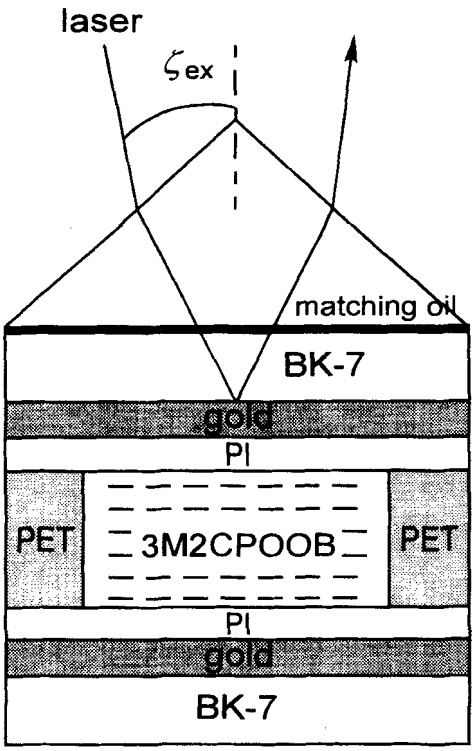

FIGURE 1 Schematic illustration of the sample cell. The thickness of each layer is listed in Table I. Two substrates face each other so that the rubbing direction is the parallel type.

were then rubbed in order to obtain planar (homogeneous) alignment of the liquid crystal. These alignment layers were prepared to have a thickness of the order of 100 nm to prevent the gold layers from frictional damages caused by the rubbing procedure. The thickness of the gold layer was determined by surface plasmon measurement and that of the PI layer by optical waveguide measurement, the details of which have been reported in a previous paper [34]. The liquid crystal was sandwiched between the two glass substrates thus obtained. The cell and a right-angle prism (BK-7) were coupled by matching oil. This sample cell was mounted on a θ–2θ goniometer (KSA-120Tθ_1–θ_2, Sigma koki) to measure the reflected intensity at an angle of incidence ζ_{ex}; the rotation of the goniometer provides angle-dependent reflectivities, *i.e.*, the waveguide mode pattern. The temperature of the cell was controlled by a thermostat (EC5500B, Ohkura) within ± 0.1°C. The optical waveguide measurement of the sample cell was performed by using *s*- and *p*-polarized light of a He–Ne laser (632.8 nm) in order to determine the dielectric tensor diagonals of the 3M2CPOOB molecules in each phase.

TROWS was conducted in the SmC* phase. An alternating rectangular electric field (typically 1 kHz frequency) was applied to the cell to induce the molecular swing of the 3M2CPOOB molecules. The time-resolving of the reflectivities from the optical cell at an incident angle ζ_{ex} was performed by using a transient memory (MR-10E, Kawasaki Electronica) with a 1.0 μs time resolution. Acquisition of the data was repeated ten times at each angle of incidence; 2 hr was needed for scanning the incident angle ζ_{ex} from 30° to 60° with a 0.1° angle increment.

3. RESULTS AND DISCUSSION

3.1. Optical Characterization of the Sample Cell

The refractive index and the thickness of each layer in the cell were precisely determined as listed in Table I. We assumed that the PI layer was optically isotropic and that the thickness of the top PI layer was the same as the bottom one. The refractive index of 3M2CPOOB and its thickness at the isotropic phase $T = 68$°C were also determined using those parameters given in Table I.

The sample geometry in that SmA phase is defined as shown in Figure 2. The rubbing direction is taken to be the X axis. In the SmA phase, 3M2CPOOB takes a bookshelf structure in which the molecules tend to

TABLE I Fitting parameters for the optical cell in the isotropic phase at $T = 68$ C

	Au(top)	*PI*	*Au(bottom)*	*3M2CPOOB*
$\varepsilon'^{[a]}$	−12.092	2.560	−12.511	2.328
$\varepsilon''^{[b]}$	1.438	0.000	1.305	0.000
$d^{[c]}$(nm)	30.5	106.9	43.5	4760

[a]The real part of the optical dielectric constant.
[b]The imaginary part of the optical dielectric constant.
[c]The thickness of the layer in the optical cell.

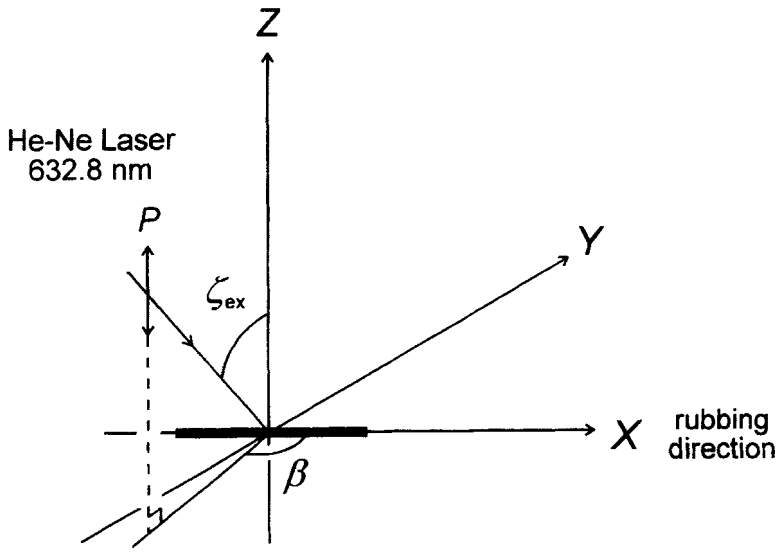

FIGURE 2 Coordinate system for 3M2CPOOB in the SmA phase used in the current study. The rubbing direction coincides with the X axis. The bold line depicts the averaged molecular direction, *i.e.*, director, which is parallel to the rubbing direction.

align parallel to the substrate and the rubbing direction, *i.e.*, the X axis. Angle β denotes the angle between the X axis and the projection of the incident light on the XY plane. The dielectric tensor of 3M2CPOOB is assumed to have only diagonal elements: ε_{xx}, parallel to the molecular long axis, and ε_{yy} and ε_{zz}, perpendicular to that. Figure 3 shows the waveguide mode patterns for (a) s light and (b) p light at $\beta = 90°$ and $T = 60°$C (SmA phase). To characterize the dielectric tensor diagonals of 3M2CPOOB in the SmA phase, the measurement was performed from two directions of the incident light: at $\beta = 90°$ perpendicular to the rubbing direction, and at $\beta = 0°$ parallel to that (not shown here). In Figure 3, the s light radiation has

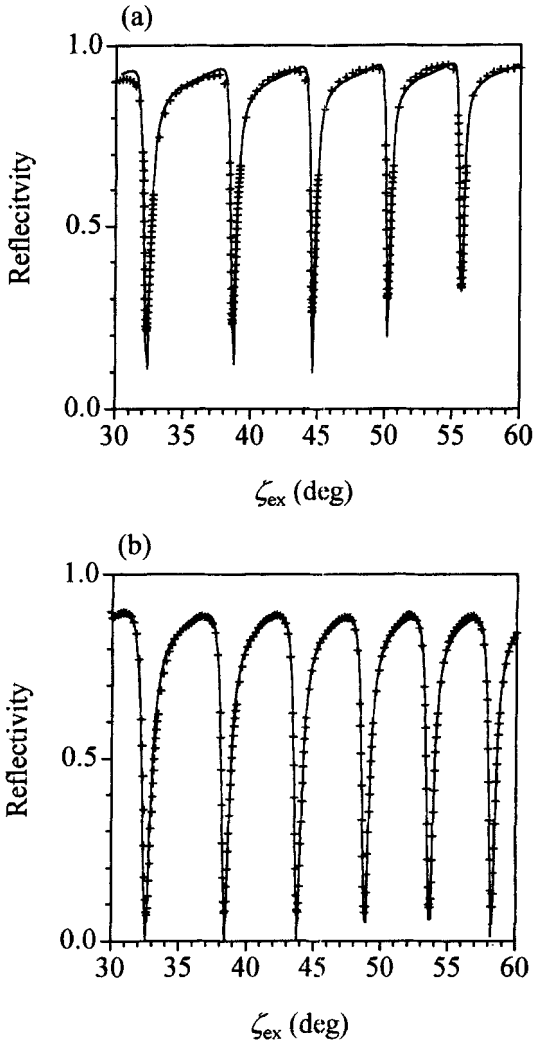

FIGURE 3 Waveguide mode patterns in the SmA phase at $T=60°C$ for (a) *s* light and (b) *p* light. The 3M2CPOOB molecules align parallel to the substrate, which means that they are arranged in the bookshelf structure. The direction of the incident light is perpendicular to the rubbing direction: $\beta = 90°$.

its *E*-field along the *X* axis, while the *p* light radiation has its *E*-field in the *YZ* plane; in both cases the dielectric tensor was orthogonalized on the plane of propagation. A series of steep dips on the reflectivity curves indicates the optical coupling of the incident beam with guided waves in the

3M2CPOOB medium, which sensitively depends on the layer thickness and the dielectric ellipsoid of 3M2CPOOB. The dielectric tensor diagonals and the thickness of the 3M2CPOOB molecules in the SmA phase at 60°C were determined from a comparison between the experimental data and the theoretical curve based on the Fresnel theory as shown with solid lines in Figure 3: $(\varepsilon_{xx}, \varepsilon_{yy}, \varepsilon_{zz}) = (2.581, 2.232, 2.232)$ and a thickness of 4.729 μm. The imaginary part of all components of the dielectric tensor diagonals could be neglected: $\varepsilon'' = 0$. These values are in good agreement with those reported previously [33].

3.2. Optical Characterization in the SmC* Phase

In the SmC* phase, the 3M2CPOOB molecules are tilted away from the smetic layer normal (the X axis). In general, without the electric field, the director of FLC molecules tends to gradually rotate layer by layer around the X axis. Consequently it shows a helical pitch toward the smectic layer normal. Additionally the layer structure is arranged from the bookshelf to the chevron structure in order to compensate the change of the density caused by the decrease of the thickness between adjacent smectic layers [7]. When a sufficiently large electric field is applied to the FLC cell, however, the helix is unwound, and then the layer structure could be deformed from the chevron to the bookshelf structure [6]. The advantage of applying the high electric field lies in the higher contrast with respect to a light beam and in the easier tractability, in particular, for the analysis of the director profile in the FLC layer. We applied a sufficiently large voltage ± 20.0 V to the 3M2CPOOB cell in order that the layer structure in the cell could turn into the bookshelf structure, and confirmed the uniform orientation under the high electric field by observation with a polarized microscope [35]. Figure 4 shows the waveguide mode patterns for p light observed at $T = 52$°C and $\beta = 90°$, that is, perpendicular to the smectic layer normal; the applied voltages were (a) -20.0 V and (b) $+20.0$ V. In this case, there exist off-diagonal components in the dielectric tensor of the FLC layer in the laboratory coordinates due to the twist of the 3M2CPOOB director from the rubbing direction. These off-diagonal components give rise to the coupling between the p- and s-polarized fields in the cell and the modes no longer have pure polarization, but merged with each other yielding additional dips as shown in Figures 4(a) and 4(b).

Normally, the spontaneous polarization of the FLC molecules, $\hat{\mathbf{P}}$, which characterizes the ferroelectricity of the medium, is defined with Eq. (1):

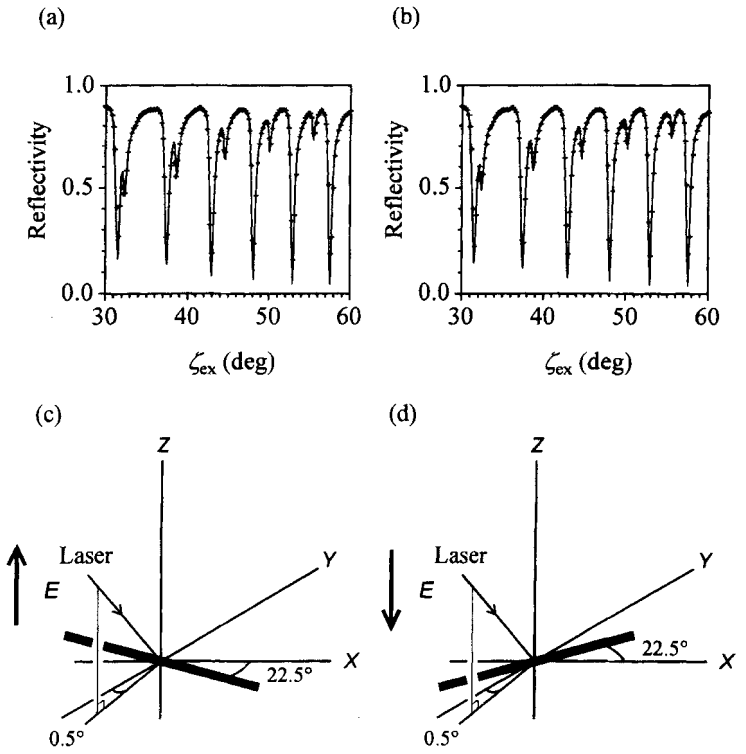

FIGURE 4 Waveguide mode patterns for p light in the SmC* phase at $T = 52°C$ measured at $\beta = 90°$. Applied voltages were (a) -20 V and (b) $+20$ V. As listed in Table II, the thickness of the 3M2CPOOB layer was evaluated as 4.700 μm. This means that the amplitudes of the applied electric field were $\pm 4.26 \times 10^4$ V/cm, which seems to be a sufficiently large electric field to change the layer structure from the chevron to the bookshelf structure.

$$\hat{\mathbf{P}} = P\frac{\hat{\mathbf{s}} \times \hat{\mathbf{n}}}{|\hat{\mathbf{s}} \times \hat{\mathbf{n}}|}, \tag{1}$$

where P is the magnitude of spontaneous polarization, $\hat{\mathbf{s}}$ the smectic layer normal, and $\hat{\mathbf{n}}$ the director of the FLC molecules. 3M2CPOOB is well known to have negative spontaneous polarization as reported previously [36]. With this fact in mind, the fitting curves (solid lines in Figs. 4(a) and 4(b)) were calculated, based on the assumption that the director lies in the XY plane through the cell, *i.e.*, the 3M2CPOOB molecules align uniformly with the bookshelf structure. The fit is in good agreement with the experimental data. The X axis must be a symmetrical axis of the molecular orientation

under the influence of an applied electric field of ± 20 V, resulting in the similarity in the shape of the waveguide mode patterns in Figures 4(a) and 4(b). Actually, we tried to adjust the probe beam direction perpendicular to the X axis, *i.e.*, $\beta = 90°$, but the real position was slightly apart from $\beta = 90°$; the error of 0.5° seems to be the limit on the setting of the cell. Anyway, the successful fit in Figures 4(a) and 4(b) indicates that the layer structure under high electric fields could be presented by the bookshelf structure model shown in Figures 4(c) and 4(d), respectively. In other words, the layer structure at the high electric field is well described by a simplified uniaxial oriented slab aligned parallel to the substrate plane. Each component of the dielectric tensor diagonals of 3M2CPOOB was summarized in Table II; the 3M2CPOOB molecules were tilted by $\pm 22.5°$ away from the smectic layer normal with the bookshelf structure under the influence of the high voltage ± 20.0 V, which was consistent with the result by polarized microscopy: 23°. The thickness of the whole FLC layer was also evaluated as 4.700 μm, which means that the amplitudes of the electric field applied to the 3M2CPOOB cell were $\pm 4.26 \times 10^4$ V/cm.

3.3. Switching Process of the 3M2CPOOB Molecules Following the Application of a Voltage Step

3.3.1. Time-Resolved Waveguide Mode Patterns for p Light Observed at $\beta = 0°$

The problem we try to solve is how the 3M2CPOOB molecules turn their orientation between the bistable bookshelf structures shown in Figures 4(c) and 4(d) at the moment of inversion of the applied voltage. Figure 5 shows the time-resolved waveguide mode patterns obtained by TROWS. The geometry for the measurement is the same as that in Figure 4. The times given on each graph in Figure 5 denote those after switching the polarity of the electric field from -20.0 V to $+20.0$ V. For a clear view, the data of $R(t)$

TABLE II Optical characterization in the SmC* phase at $T = 52$°C. The thickness of the 3M2CPOOB layer was evaluated as 4.700 μm. This means that the amplitudes of the applied electric field were $\pm 4.26 \times 10^4$ V/cm

	ε_{xx}	ε_{yy}	ε_{zz}	ϕ (deg)	θ (deg)
-20 V	2.628	2.228	2.228	0	22.5
$+20$ V	2.628	2.228	2.228	180	22.5

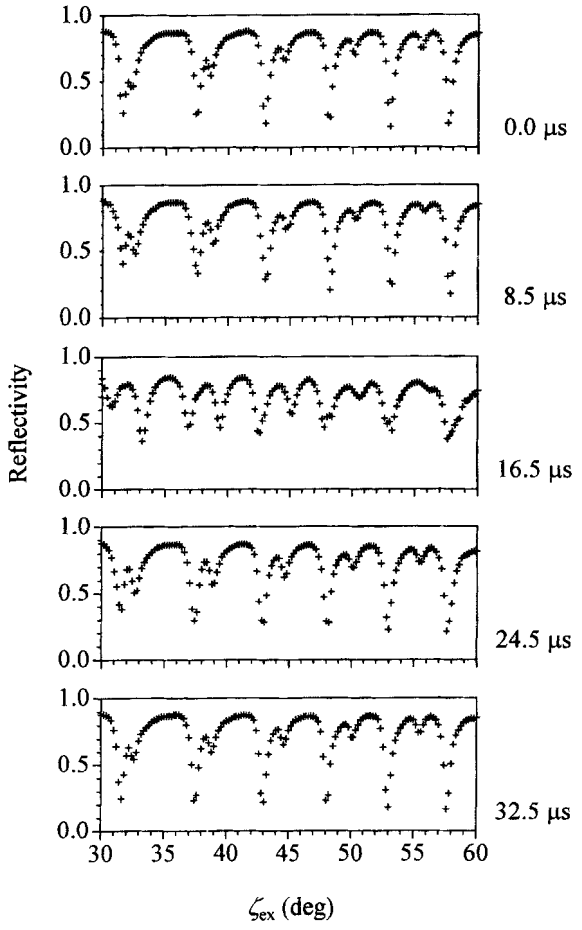

FIGURE 5 Time-resolved waveguide mode patterns for p light in the SmC* phase at $T = 52°C$. An alternating electric field, 40 V_{pp} and 1 kHz frequency, was applied to the cell to induce the molecular reorientation between the bistable bookshelf structures. The times on each graph denote those after the polarity of the electric field changes from minus to plus.

every ca. 8.0 μs were shown in Figure 5. These waveguide mode patterns plainly show the shift of the angular position for each optical mode with the elapse of time. As mentioned earlier, the director of the 3M2CPOOB molecules is tilted away from the X axis in the XY plane, therefore the birefringence effect must be taken into account. The odd peaks from the left side in all graphs are p light-like modes, while the even peaks are s light-like modes originated from the strong p–s coupling in the 3M2CPOOB layer. Focusing

on the two dips at the smaller angles in Figure 5, it is clear that the reflectivity at the position of the *p* light-like mode (left dip) initially increases within around 15 μs and then decreases as the 3M2CPOOB molecules get close to the other orientation; on the other hand, the situation for the *s* light-like mode (right dip) was opposed to that of the *p* light-like mode. In other words, the molecular motion of the 3M2CPOOB molecules was transfigured into a change in the shape of the waveguide mode pattern. And this also indicates that the time-resolved waveguide mode patterns have the potential of probing the dynamics of transition through TROWS with microsecond time resolution.

3.3.2. Angle Definition and Some Assumptions to Describe the Reorientation of the 3M2CPOOB Molecules

Now our purpose is to analyze each transient waveguide mode pattern using some reorientation models and to make clear the kinetics of the reorientation of 3M2CPOOB molecules.

It is necessary to define three angles which describe the orientation of the director of 3M2CPOOB molecules in the SmC* phase with respect to the laboratory coordinate system as shown in Figure 6. Three angles (θ, ϕ, ψ)

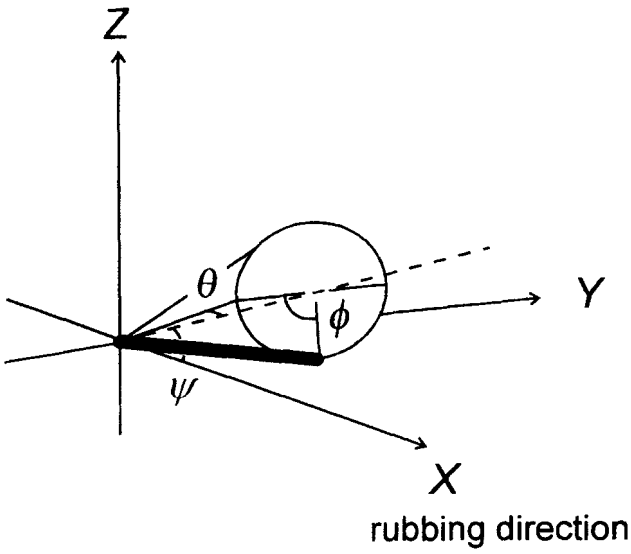

FIGURE 6 Angle definition of the director in order to describe the molecular reorientation. Three angels, θ, ϕ and ψ are given in the figure; θ, the angle between the director and the cone axis, ϕ, the azimuthal angle of the director on the cone, and ψ, the angle of the cone axis away from the X axis in the XZ plane.

denote the cone angle θ, the azimuthal angle ϕ, and the layer tilt angle ψ. The azimuthal angle ϕ increases from 0° to 180° around the smectic cone. The layer tilt angle ψ is given by the angle between the X axis and the cone axis in the XZ plane; the larger ψ the greater deformation from the bookshelf structure to the chevron one.

To figure out the experimental data, we made some assumptions as follows:

1. The 3M2CPOOB cell was divided into two parts, half and half to the direction of the film thickness. The calculation of the angle-dependent reflectivity was performed for this two-layer structure, where the top and bottom halves have their own rotational parameters. The treatment allows for the possibility of the chevron structure formation during the molecular reorientation.
2. The 3M2CPOOB molecules reorient simultaneously in each layer, *i.e.*, both the azimuthal angle ϕ and the layer tilt angle ψ at a given time are constant throughout each layer during the reorientation.
3. The sum of the components of the dielectric tensor diagonals is kept constant and the dielectric tensor of the 3M2CPOOB molecules is regarded as a uniaxial dielectric ellipsoid model during the reorientation.

Numerical calculation of the angle-dependent reflectivity based on these assumptions was executed using the modified Berreman's 4×4 matrix [37] method, the procedure of which has been reported previously [18].

3.3.3. Rotational Direction of the 3M2CPOOB Molecules

First we tried to find a suitable model for the route through which the 3M2CPOOB molecules move. Figures 7(a) and 7(b) show the rotational motion of the director induced by the voltage step; the arrows point in the same direction in Figure 7(a), *i.e.*, the 3M2CPOOB molecules reorient cooperatively throughout the cell, while in Figure 7(b), they reorient in opposite between the top and the bottom halves of the cell. In this case, the directions in both the two layers in Figure 7(b) point to the middle of the cell. Cross points in Figures 7(c) and 7(d) represent the experimental data at $t = 25.5$ μs after the electric field reversal from -20.0 V to $+20.0$ V. The solid lines in Figures 7(c) and 7(d) are the fit calculated with the models in Figures 7(a) and 7(b), respectively. Noticeable differences are observed between Figures 7(c) and 7(d), in particular, in the smaller angles of incidence. There are two more plausible routes [38] for the rotational motions (not shown here), but only the one drawn in Figure 7(b) gave the acceptable fit.

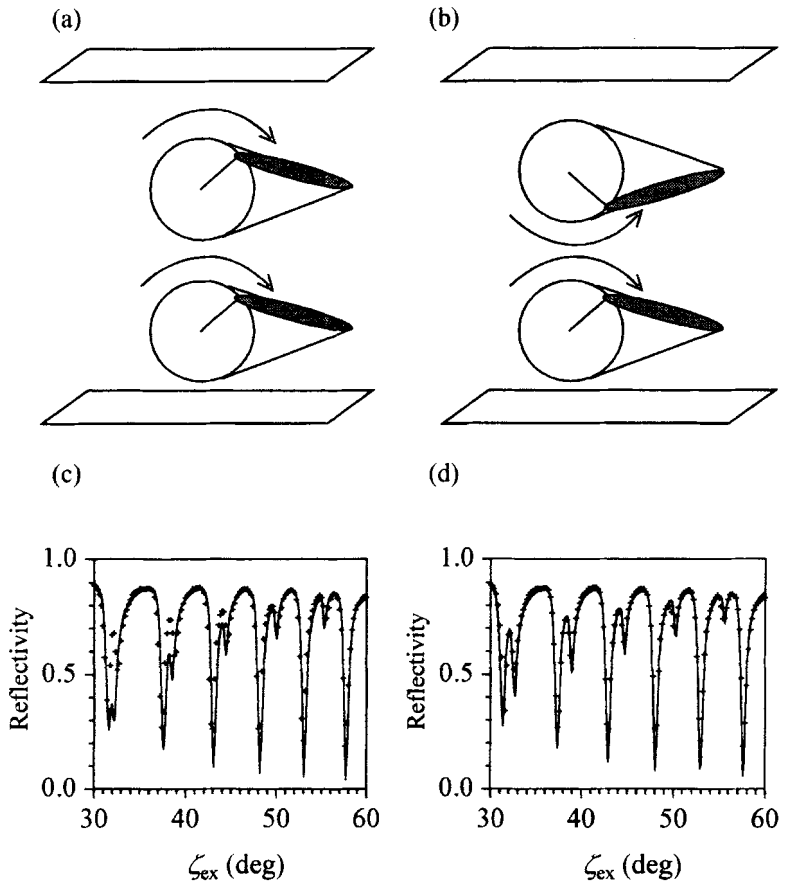

FIGURE 7 Two possible rotational models: (a) the 3M2CPOOB molecules rotate with the same direction around the smectic cone through the 3M2CPOOB layer, (b) they undergo counter rotations between the top and the bottom halves of the layer; (c) and (d) fitting results for the transient waveguide mode pattern at $t = 25.5$ μs. These fittings were carried out using the model as shown in (a) and (b), respectively.

If the layer holds the bookshelf structure during the switching motion, no difference among these rotational models would be observed in the fitting. The layer tilt angle ψ has a remarkable effect on the resonance angles of the optical waveguide modes, even if the amount ψ is only 1° in the top and $-1°$ in the bottom layers. That is why the differences in these rotational models could be distinguished. The opposite sign between the top and bottom layers means that the smectic layer bends at the middle of the cell like the chevron during the reorientation. The counter rotation might result

from the influence of the surface of the alignment polymers [39]. Sambles *et al.*, proposed another requirement for the counter rotation: the optic tensor profile must retain the continuity at the chevron cusp [13]. Moreover, considering the electrostatic interaction between the spontaneous polarization and the opposite electric field under the chevron structure, the counter rotation is preferred from the view of energy minimization [4]. These speculations could be proved by the measurement of TROWS. The most outstanding result is the finding that the progress of the switching motion could be observed with the microsecond range resolution, indicating again that TROWS is capable of probing the dynamics of the directors and the transient layer structure of the FLC.

3.3.4. The Dependence of $\Delta R(t)$ on the Layer Tilt Angle ψ

To investigate the kinetics of the switching process in more detail, let us introduce the change of reflectivity, $\Delta R(t)$ as defined by Eq. (2):

$$\Delta R(t) = R(t) - R(0), \tag{2}$$

where $R(0)$ is the reflectivity just before switching of the E-field. Figure 8 shows the layer tilt dependence of $\Delta R(t)$ at $t = 15.5$ μs after the electric field reversal at $t = 0.0$ μs. The experimental plots (+) are the same in all graphs, but the theoretical curves $\Delta R(t)$ shown with solid lines were calculated by changing the layer tilt angle ψ. We used the optical parameters listed in Table II for the calculation of $R(0)$, and the dielectric tensor diagonals at 15.5 μs were fixed through all graphs in Figure 8 as described in the figure caption. The time 15.5 μs corresponds to the halfway point of the switching process. Figure 8(a) is the result for the case of $\psi = 0°$, in which the smectic layer does not tilt from the surface normal, *i.e.*, holding the bookshelf structure during the switching process. Obviously, this is not the case. This result signifies that the 3M2CPOOB molecules move around the cone, but that the cone itself is not constrained to the bookshelf structure. Figures 8(b), 8(c) and 8(d) show the dependence of $\Delta R(t)$ on the layer tilt angle ψ:ψ = (b) 4.0° (c) 7.5°, and (d) 12.0°, respectively; the layer is tilted away from the substrate normal by a positive angle in the top layer, while by a negative angle in the bottom layer. As observed at the lower part of $\Delta R(t)$, there are clear discrepancies in the position of the modes between the theoretical curve and the experimental data shown in Figures 8(b) and 8(d) as well as in Figure 8(a). The theoretical curve in Figure 8(c) is in good agreement with the experimental data. In other words, when the 3M2CPOOB

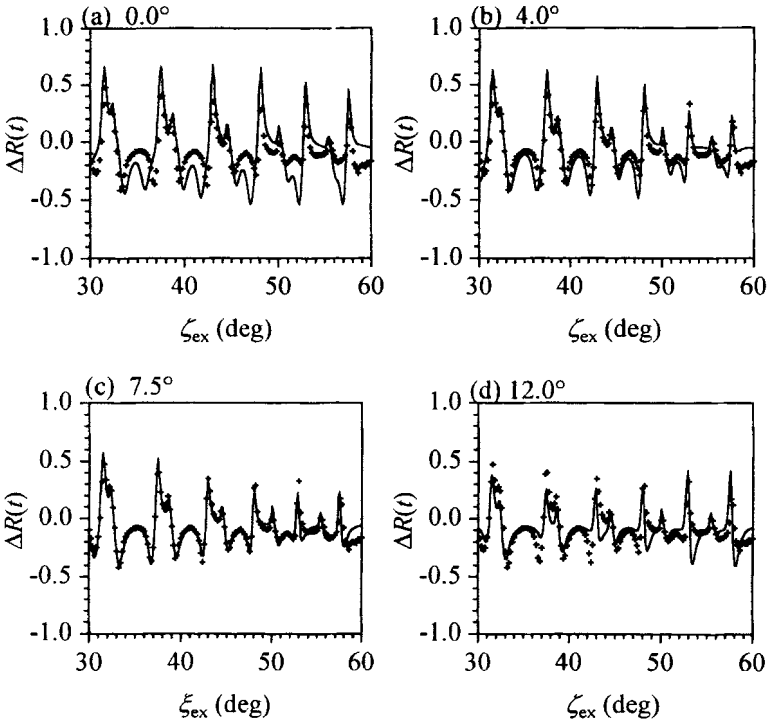

FIGURE 8 The layer tilt angle dependence of the reflectivity change $\Delta R(t)$: $t = 15.5$ μs. The dielectric tensor diagonals at $t = 15.5$ μs were fixed: $(\varepsilon_{xx}, \varepsilon_{yy}, \varepsilon_{zz}) = (2.603 + 0.007i,\ 2.241 + 0.007i,\ 2.241 + 0.007i)$. The layer tilt angle ψ was changed from (a) 0.0° to (d) 12.0°. The magnitude of the tilt angle is the same in the top and bottom layers, but the sign is opposite, which indicates the existence of a chevron-like structure during the reorientation.

molecules reorient from one direction to the other around the cone, overall smectic layer buckling takes place during switching: $\psi = 7.5°$ at 15.5 μs. This finding implies that the reorientation of the 3M2CPOOB molecules induced by the high electric field reversal is caused by the coupling of the layer deformation and the rotational motion around the cone. The buckling phenomenon was successfully detected with the change of reflectivity coupled with the guided waves, showing the high sensitivity for the molecular dynamics in the FLC layer.

3.3.5. The Effect of the Dielectric Tensor on $\Delta R(t)$

Figure 9 represents the effect of the dielectric tensor diagonals of the 3M2CPOOB molecules on $\Delta R(t)$ at $t = 15.5$ μs. The experimental data all in

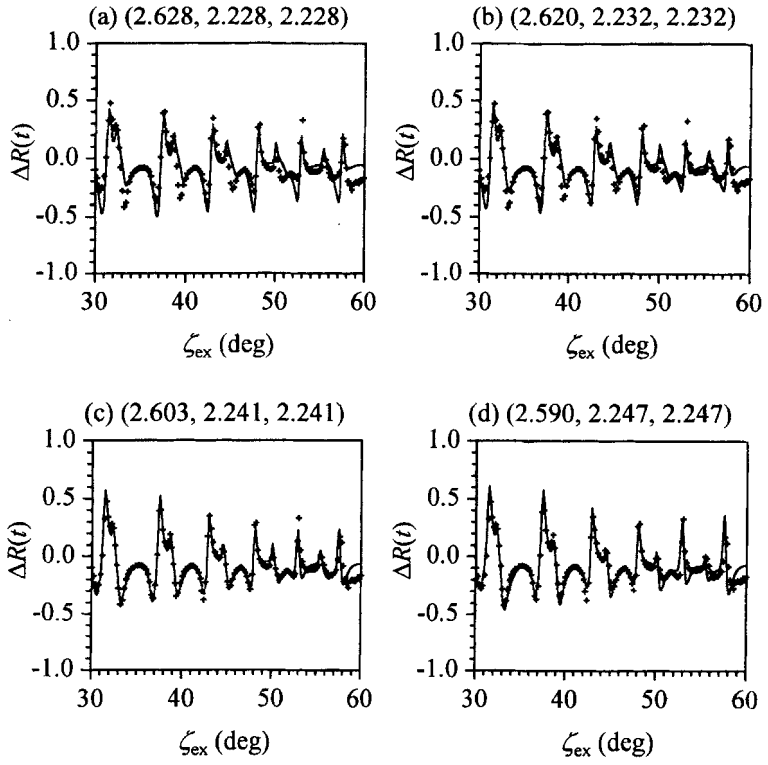

FIGURE 9 The dependence of $\Delta R(t)$ on the dielectric tensor diagonals. The layer tilt angle ψ was fixed at $\psi = 7.5°$. The magnitudes of the diagonals were changed as follows: (ε_{zz}, ε_{yy}, ε_{zz}) = (a) (2.628, 2.228, 2.228), (b) (2.620, 2.232, 2.232), (c) (2.603, 2.241, 2.241) and (d) (2.590, 2.247, 2.247). The best fit is Figure 9(c). The magnitude of the components in Figure 9(a) is the same as that of the initial state at $t = 0.0\,\mu s$. The theoretical curve in Figure 9(c) is the same as that in Figure 8(c).

Figure 9 are the same as those in Figure 8. We changed the real part of the dielectric tensor diagonals keeping the sum of components constant, whereas the imaginary part of the dielectric constants was set at 0.007: (ε_{xx}, ε_{yy}, ε_{zz}) = (a) (2.628, 2.228, 2.228), (b) (2.620, 2.232, 2.232), (c) (2.603, 2.241, 2.241), and (d) (2.590, 2.247, 2.247). The layer tilt angle ψ was fixed at 7.5°. As the dielectric tensor changes, the theoretical curve $\Delta R(t)$ also alters its shape, giving distinct differences in the intensity, in particular at the peaks between the theoretical curves and the experimental data, except for Figure 9(c). The diagonals used in Figure 9(a) are the same as those of the initial state listed in Table II, which means that the 3M2CPOOB molecules would rotate around the cone with no change of the dielectric constants. However the

theoretical curve is not in good agreement with the experimental data in Figure 9(a). Figure 9(c) is the same as Figure 8(c), showing the best fit with the experimental data, that is to say, the dielectric tensor slightly changes during the reorientation. As for ε_{xx}, the difference from the initial state was evaluated to be a decrease of 0.025, whereas $\Delta\varepsilon_{yy}$ and $\Delta\varepsilon_{zz}$ were increases of 0.013. This finding indicates that the component of the diagonals ε_{xx} is decreasing within 15 μs and then increasing back to the original value, while the opposite is the case for y and z components of the dielectric tensor diagonals. In other words, the 3M2CPOOB molecules undergo cooperative motions but they are not perfect, having some orientational distribution during the reorientation from one direction to the other. One possible explanation for this is that the 3M2CPOOB molecules have some velocity distribution during the reorientation. This distribution appears as the deformation of the dielectric ellipsoid on average; at the initial stage of rotation it shrinks along with the molecular long axis, while it enlarges toward the direction perpendicular to the molecular long axis. Another possibility is that the reversal of the external electric field may affect the spontaneous polarization of the 3M2CPOOB molecules, which weakens the dielectric components of the molecular long axis. This explanation is based on the fact that the cone angle θ becomes larger as the external field is increased, *i.e.*, the dipole moment of the 3M2CPOOB is more oriented with the increase of the external field, resulting in the change of the dielectric tensor on average. However such a small readjustment of directors must take place within a very short time following the voltage step in the nanosecond region. Considering the time range we observed, a few tens of microseconds, the former velocity distribution is likely to be a reasonable explanation for the transient shrinkage of the dielectric tensor.

To avoid confusion, it should be again noted that the change of the dielectric diagonals is just apparent one on average and does not mean that the dielectric diagonals of the 3M2CPOOB molecule change during reorientation. We divided the 3M2CPOOB layer into two regions, and the values used herein correspond to the average dielectric diagonals in each region. Therefore the change of the apparent dielectric diagonals implies that the orientation of the 3M2CPOOB molecules has some kind of distribution during the reorientation process. As for the cause, we suggested the velocity distribution of the directors during the reorientation. However a similar result may be caused by the distribution of the azimuthal angle as a function of the displacement of the Z axis due to the surface effect from the substrates. Both have a very similar effect on the reflectivity curves, and we cannot distinguish these two possibilities. But taking into account both

the high electric field and the simultaneous appearance of the imaginary part mentioned in the later section, the velocity distribution seems to be responsible for the apparent change of diagonals.

The fitting results for the time-resolved waveguide mode patterns are shown in Figure 10. The theoretical curves are in fairly good agreement with all experimental data, in particular, at the position of each mode between the theoretical curve and the experimental data over the whole

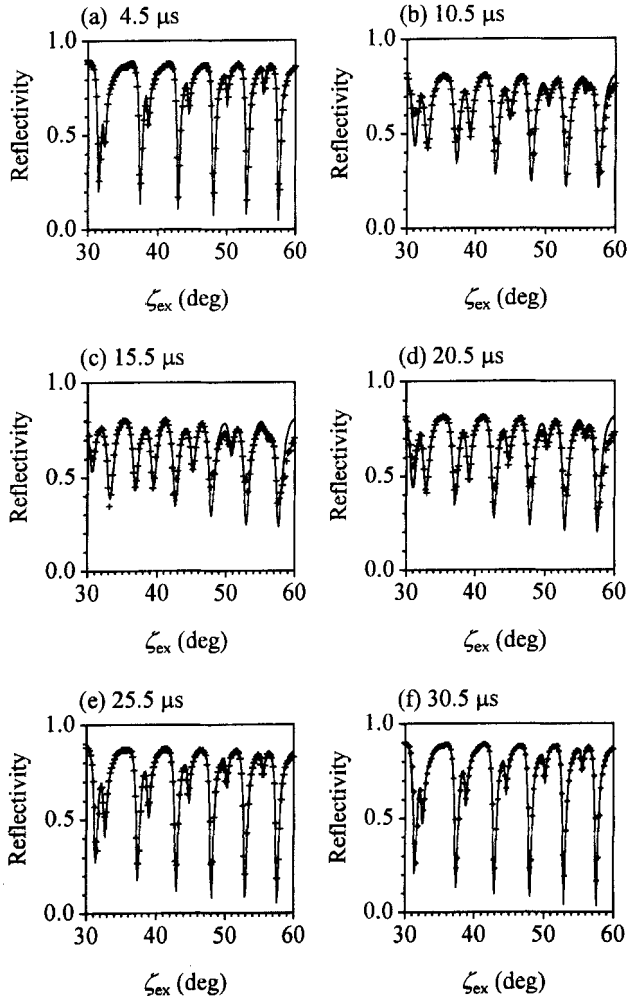

FIGURE 10 Overall fitting results for the transient waveguide mode patterns for *p*-light at $\beta = 90°$ from (a) 4.5 μs to (f) 30.5 μs.

time range and the wide angle of incidence. This result supports the validity of the simple description for the switching process mentioned above.

3.4. A Dynamic Model of the 3M2CPOOB Molecules in the Course of the Switching Process

Figure 11 shows the time dependence of each parameter used in the fitting: (a) the azimuthal angle ϕ, (b) the layer tilt angle ψ. As shown in Figure 11(a), it is clear that the reorientation of the 3M2CPOOB molecules was completed within 30 μs induced by the large voltage step of 8.52×10^4 V/cm. Xue *et al.* [40] reported the time evolution of the azimuthal angle ϕ

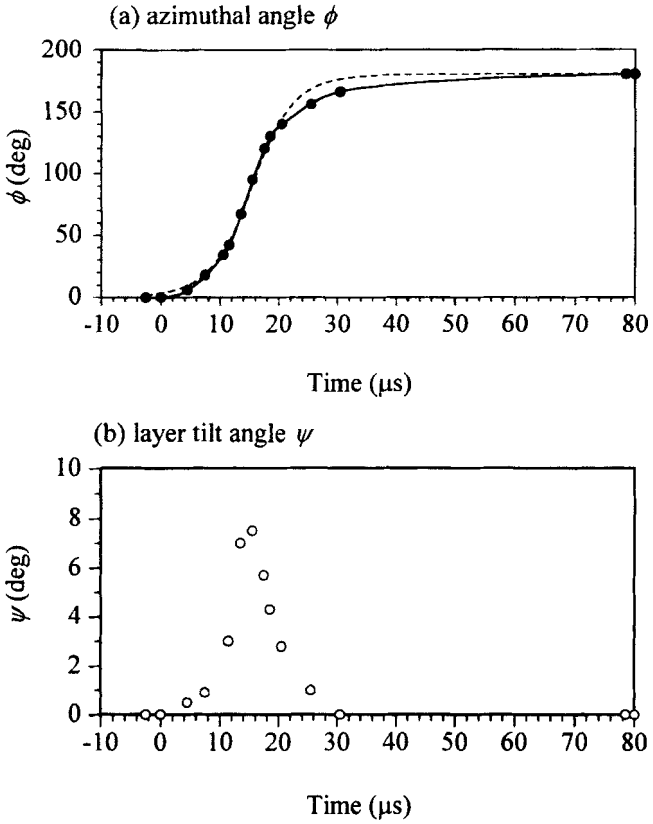

FIGURE 11 Time dependence of (a) azimuthal angle ϕ and (b) layer tilt angle ψ. The solid line in (a) was obtained from Eq. (4) which gives better fitting than the dashed line optimized from Eq. (5), which means that under a high electric field the contribution from the dielectric anisotropy must be taken into consideration as well as that from the ferroelectric interaction.

derived from Eq. (3), neglecting the contribution from the moment of inertia and the surface interaction:

$$\eta \frac{d\phi}{dt} = PE\sin\phi + \left(\frac{\Delta\varepsilon}{4\pi}\right)E^2 \sin^2\theta \sin\phi \cos\phi, \tag{3}$$

where η is the rotational viscosity, $\Delta\varepsilon$ the dielectric anisotropy at low frequency, E the electric field applied to the liquid crystal cell and P the magnitude of spontaneous polarization. The solid line in Figure 11(a) was obtained using Eq. (4), which is the solution of Eq. (3):

$$t/\tau = \frac{1}{1-\alpha^2}\left\{\ln\frac{\tan(\phi/2)}{\tan(\phi_0/2)} + \alpha \ln\left[\frac{(1+\alpha\cos\phi)\sin\phi_0}{(1+\alpha\cos\phi)\sin\phi}\right]\right\}, \tag{4}$$

where $\tau = \eta/PE$, $\phi_0 \equiv \phi(t=0)$, and $\alpha = \Delta\varepsilon E\sin^2\theta/(4\pi P)$. The line calculated with $\tau = 4.2\,\mu s$, $\phi_0 = 0.9°$, and $\alpha = 0.52$ seems in good agreement with the experimental data [41], whereas the contribution of the layer tilt angle ψ is neglected in Eq. (3). This is not surprising due to the following consideration. The contribution of ψ to two right terms of Eq. (3) is $\cos\psi$ and $\cos^2\psi$, respectively [15]. In the present case, the maximum layer tilt angle was $\psi = 7.5°$, at which the values of $\cos\psi$ and $\cos^2\psi$ are 0.99 and 0.98; the contribution of these terms of Eq. (3) is negligible.

The dashed line was the calculated curve including only the contribution from the ferroelectric torque; the solution was given by Eq. (5), which gives poorer fitting than that of Eq. (4):

$$\frac{t}{\tau} = \ln\frac{\tan(\phi/2)}{\tan(\phi_0/2)}. \tag{5}$$

The parameters were obtained from the least square optimization as follows: $\phi_0 = 3.4°$ and $\tau = 4.4$ (μs). This means that the contribution not only from the ferroelectric torque, but also from the dielectric torque must be considered under the high electric field. In other words, under a high electric field, the contribution from the dielectric anisotropy cannot be neglected, which slows down the time of switching.

Figure 11(b) indicates that the 3M2CPOOB molecules undergo the layer buckling motion during the reorientation from one direction on the smectic cone toward the other side of the cone; both the initial and final states are

the bookshelf structure. Two effects are conceivable as the reason for this: one is the relaxation from the bookshelf to the chevron structure, and the other the anti-parallel interaction between the spontaneous polarization and the electric field as described in section 3.3.3 [4]. The former may be caused by the interaction between the surface and the 3M2CPOOB molecules. We neglect the surface effect on the fitting, but this problem should be clarified in the future.

Figure 12 shows the time dependence of (a) the real part of the dielectric constant (ε_{xx}, ε_{yy}, ε_{zz}) and (b) the apparent imaginary part of the dielectric constant. The real part of the dielectric tensor diagonals along with the molecular long axis changed once to decreasing and then increasing toward

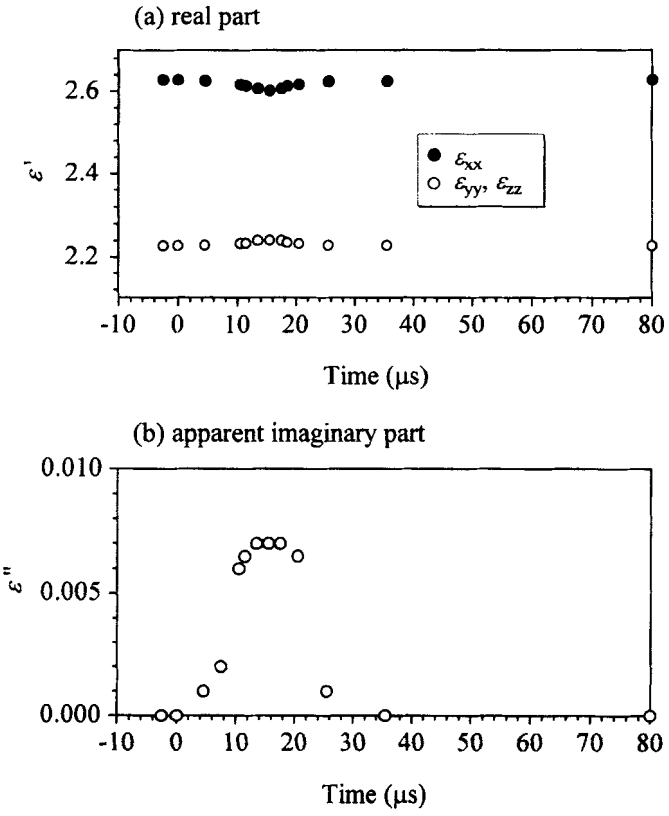

FIGURE 12 Time dependence of the dielectric tensor diagonals: (a) the real part and (b) the apparent imaginary part. (a) The component of the molecular long axis ε_{xx} is once decreasing, and then increasing to the orignal value, while the opposite situation is the case of ε_{yy} and ε_{zz}. (b) The maximum apparent imaginary part is 0.007 which might be caused by the light scattering during the reorientation.

the original value. As shown in Figure 12(b), the change in the apparent imaginary part of the dielectric diagonals during reorientation must be taken into account, even though the value is small compared with the case of a nematic liquid crystal [30]. The light scattering during the reorientation is the most plausible cause for it. This may be also responsible for the slight deviation between the theoretical and the experimental data in the transient reflectivities in Figure 10. As for the light scattering, the disclination during the reorientation observed under a low electric field by a stroboscopic microscope may be one of the responsible factors [26]. We simplified the switching process by the use of a high electric field so that the discontinuity can apparently be neglected. But the discontinuity resulting from the nucleation of the disclination may occur even under a high electric field. This could be a reason for the discrepancy between the experimental data and the theoretical curve, in particular, during the transient states near the midpoint of the molecular motion.

From these considerations, a reorientation model of the 3M2CPOOB molecules between two stable bookshelf structures under a high electric field is proposed as illustrated in Figure 13; (a) intially 3M2CPOOB molecules

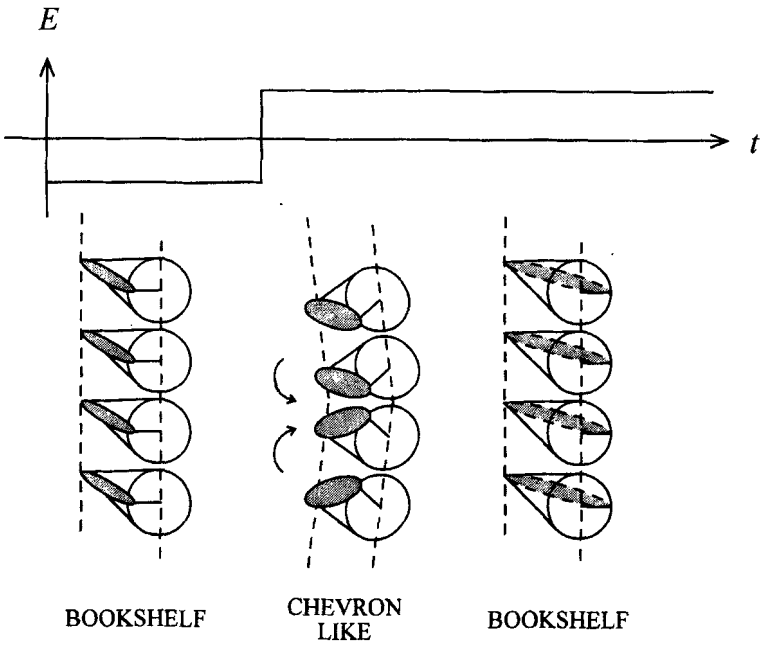

FIGURE 13 Schematic drawing for the molecular reorientation of the 3M2CPOOB induced by the large voltage step.

orient along one direction with a bookshelf structure under the high electric field. When the polarity is changed, (b) the molecules start moving with counter rotation between the top and the bottom halves of their layers. Simultaneously, the smectic layers bend from the substrate normal, and then (c) the 3M2CPOOB molecules achieve the other orientation again with the bookshelf structure. During the reorientation, all the 3M2CPOOB molecules rotate uniformly, but having some orientational distribution.

4. CONCLUSION

Time-resolved optical waveguide spectroscopy was utilized to investigate the switching dynamics of the ferroelectric liquid crystal molecules (3M2CPOOB) under an alternating electric field. The changes of both the tensor diagonals of 3M2CPOOB and the angles which defined the direction of the director in the laboratory coordinate system were successfully detected using TROWS with a 1.0 μs time-resolution. From the quantitative analysis of the transient waveguide mode patterns, a reorientation model was proposed as follows: the molecular motion around the cone is coupled with the layer buckling, involving some orientational distribution which results in the transient shrinkage of the dielectric ellipsoid. This implies that the 3M2CPOOB molecules take a chevron-like structure during the reorientation from one bookshelf structure to the other. The rotation represented by the azimuthal angle under the high electric field could be described with the equation of director rotation based on a ferroelectric torque and a dielectric torque. Of course, these molecular motions may be greatly influenced by the properties of the materials, the surface treatment, and the manner of application of the electric field, *etc.* As shown in the present discussion, TROWS enables us to investigate the dynamic structure and reorientation kinetics of the FLC molecules in the microsecond time range.

Acknowledgments

The authors thank Dr. F. Kremer for providing the present sample. The authors further wish to thank Professor A. Fukuda for his various comments and fruitful discussion about our results. This work was supported by a Grant-in-aid for Scientific Research (No. 07651105) by the Ministry of Education, Science, Sports, and Culture of Japan. M. Mitsuishi would like

to thank the Japan Society for the Promotion of Science for a Research Fellowship.

References

[1] N. A. Clark and S. T. Lagerwall, *Appl. Phys. Lett.*, **36**, 899 (1980).
[2] M. H. Anderson, J. C. Jones, E. P. Raynes and M. J. Towler, *J. Phys. D.*, **24**, 338 (1991).
[3] T. C. Chieu, K. H. Yang and A. Lien, *J. Appl. Phys.*, **64**, 6654 (1988).
[4] W. J. A. M. Hartmann, G. Vertogen, C. J. Gerritsma, H. A. v. Sprang and A. G. H. Verhulst, *Europhys. Lett.*, **10**, 657 (1989).
[5] T. P. Rieker, N. A. Clark, G. S. Smith, D. S. Parmar, E. B. Sirota and C. R. Safinya, *Phys. Rev. Lett.*, **59**, 2658 (1987).
[6] M. Isogai, M. Oh-e, T. Kitamura and A. Mukoh, *Mol. Cryst. Liq. Cryst.*, **207**, 87 (1991).
[7] For example, (a) R. Blinc, N. A. Clark, J. W. Goodby, S. A. Pikin and K. Yoshino, *Ferroelectric Liquid Crystals* (Gordon and Breach, New York, 1984); (b) A. Fukuda and H. Takezoe, *Structures and Properties of Ferroelectric Liquid Crystal* (Corona, Tokyo, 1990 (in Japanese)); (c) R. Blinc and B. Zeks, *Ferroelectric and Antiferroelectric Liquid Crystals and Their Electrooptic Applications* (World Scientific, Singapore, 1995).
[8] W. Knoll, *Mater. Res. Bull.*, **16**, 29 (1991).
[9] W. Knoll, *Makromol. Chem.*, **192**, 2827 (1991).
[10] E. F. Aust, S. Ito, M. Sawodny and W. Knoll, *Trends Polym. Sci.*, **2**, 313 (1994).
[11] P. K. Tien, *Rev. Mod. Phys.*, **49**, 361 (1977).
[12] S. J. Elston and J. R. Sambles, *Jpn. J. Appl. Phys.*, **29**, 641 (1990).
[13] S. J. Elston and J. R. Sambles, *Mol. Cryst. Liq. Cryst.*, **200**, 167 (1991).
[14] S. J. Elston and J. R. Sambles, *Mol. Cryst. Liq. Cryst.*, **220**, 99 (1992).
[15] S. J. Elston, *J. Mod. Opt.*, **42**, 19 (1995).
[16] F. Yang and J. R. Sambles, *J. Opt. Soc. Am. B.*, **10**, 858 (1993).
[17] D. Y. K. Ko and J. R. Sambles, *J. Opt. Soc. Am. A.*, **5**, 1863 (1988).
[18] S. Ito, F. Kremer, T. Fischer and W. Knoll, *Mol. Cryst. Liq. Cryst.*, **264**, 99 (1995).
[19] J. E. Maclennan, M. A. Handschy and N. A. Clark, *Phys. Rev. A.*, **34**, 3554 (1986).
[20] Y. Ouchi, H. Takano, H. Takezoe and A. Fukuda, *Jpn. J. Appl. Phys.*, **26**, L21 (1987).
[21] F. Gießelmann and P. Zugenmaier, *Liq. Cryst.*, **14**, 389 (1993).
[22] J. Abdullhalim, G. Moddel and N. A. Clark, *J. Appl. Phys.*, **76**, 820 (1994).
[23] (a) M. A. Czarnecki, N. Katayama, Y. Ozaki, M. Satoh, K. Yoshino, T. Watanabe and T. Yanagi, *Appl. Spectrosc.*, **47**, 1382 (1993); (b) S. V. Shilov, S. Okretic, H. W. Siesler and M. A. Czarnecki, *Appl. Spectrosc. Rev.*, **31**, 125 (1996).
[24] K. Nito, H. Takanashi and A. Yasuda, *Liq. Cryst.*, **19**, 653 (1995).
[25] Y. Ouchi, H. Takezoe and A. Fukuda, *Jpn. J. Appl. Phys.*, **26**, 1 (1987).
[26] K. H. Kim, K. Ishikawa, H. Takezoe and A. Fukuda, *Phys. Rev. E.*, **51**, 2166 (1995).
[27] T. S. Perova, Y. P. Panarin and J. K. Vij, *Ferroelectrics*, **180**, 105 (1996).
[28] (a) H. J. Coles and J. Tipping, *Nature*, **316**, 136 (1985); (b) J. M. W. Hanmer and H. J. Coles, *Mol. Cryst. Liq. Cryst.*, **262**, 235 (1995).
[29] M. Mitsuishi, S. Ito, M. Yamamoto and W. Knoll, *Appl. Phys. Lett.*, **69**, 2199 (1996).
[30] M. Mitsuishi, S. Ito, M. Yamamoto, T. Fischer and W. Knoll, *J. Appl. Phys.*, **81**, 1135 (1997).
[31] K. Yoshino, M. Ozaki, S. Kishio, T. Sakurai, N. Mikami, R. Higuchi and M. Honma, *Mol. Cryst. Liq. Cryst.*, **144**, 87 (1987).
[32] S. U. Vallerien, F. Kremer, H. Kapitza, R. Zentel and W. Frank, *Phys. Lett. A.*, **138**, 219 (1989).
[33] S. Ito, F. Kremer, E. Aust and W. Knoll, *J. Appl. Phys.*, **75**, 1962 (1994).
[34] G. J. Sprokel, *Mol. Cryst. Liq. Cryst.*, **68**, 39 (1981).
[35] When we applied a sufficiently high electric field to the cell, the textures observed under a polarized microscope were drastically changed to striped-like patterns ((a) M. Johno, Y. Ouchi, H. Takezoe, A. Fukuda, K. Terashima and K. Furukawa, *Jpn. J. Appl. Phys.*, **29**, L111, (1990); (b) R. F. Shao, P. C. Willis and N. A. Clark, *Ferroelectrics*, **121**, 127

(1991); (c) L. L. Bournis and L. Dupont, *Ferroelectrics*, **149**, 69 (1993).). This means that the layer structure changed from the chevron structure to the bookshelf structure. The in-plane orientation caused by the layer deformation would be complicated, but we simplified it as a uniform orientation, because we detected the light reflected from the cell on average over the whole thickness.

[36] J. S. Patel and J. W. Goodby, *Opt. Eng.*, **26**, 373 (1987).

[37] D. W. Berreman, *J. Opt. Soc. Am.*, **62**, 502 (1972).

[38] One is simultaneous rotation as the initial rotational direction is upward. The other is counter rotation between the top and bottom halves of FLC layer where the rotational direction is upward in the top and downward in the bottom FLC layer.

[39] K. Ishikawa, T. Uemura, H. Takezoe and A. Fukuda, *Jpn. J. Appl. Phys.*, **24**, L230 (1985).

[40] J. Z. Xue, M. A. Handschy and N. A. Clark, *Ferroelectrics*, **73**, 305 (1987).

[41] We could not evaluate P and $\Delta\varepsilon$ separately, but as for the sign for $\Delta\varepsilon$, the result was plus. This is the same result as Ref. 42. As a matter of fact, the sample used therein was 4-(2*S*, 3*S*)-[2-chloro-3-methylpentanoyloxy]-4′-heptyloxybiphenyl, the molecular structure of which is quite similar to our sample.

[42] E. I. Demikhov, S. A. Pikin and E. S. Pikina, *Phys. Rev. E.*, **52**, 6250 (1995).